A CASE STUDY IN THE CAPACITY DESIGN OF RC COUPLED WALLS

Matthew J. FOX[1], Timothy J. SULLIVAN[2] and Katrin BEYER[3]

ABSTRACT

In the seismic design of structures, capacity design is typically employed to ensure that a desirable ductile response is obtained. In this paper three different capacity design approaches for reinforced concrete coupled walls are investigated. For a simple case study building, the expected capacity design shear forces and bending moments are calculated using the different approaches. The results are then assessed against the corresponding actions found from nonlinear time-history analysis. The performance of each approach is discussed, along with some of the difficulties associated with undertaking the capacity design of coupled walls.

INTRODUCTION

Reinforced concrete (RC) coupled walls are a structural system commonly used in buildings to resist lateral loads induced by wind and seismic actions. They consist of two or more individual walls linked by coupling beams up the height of the building, most commonly at every floor level. The coupling effect induces axial forces in the walls and therefore the overturning moment is resisted by two separate mechanisms; (i) moment resistance at the base of the walls, and (ii) the axial force couple generated by the coupling. This paper looks at the capacity design of such walls and in particular focuses on higher mode effects.

The philosophy of capacity design (Park and Paulay, 1975; Paulay and Priestley, 1992), incorporated into the seismic design of structures, ensures that during an earthquake the structure responds in a favourable ductile manner. This is done by pre-selecting a suitable plastic mechanism and then providing special detailing to the plastic hinge regions so that they may dissipate energy under severe imposed displacements. Undesirable failure modes, such as shear failure, are suppressed by providing them with a strength greater than that corresponding to the development of the maximum feasible strength in the plastic hinge regions.

In this paper a number of existing capacity design approaches are applied to a case study coupled wall building. The performance of each approach is then evaluated against the actions obtained from nonlinear time-history analyses (NTHA). In the first section, the case study building is described, including key aspects of its seismic design. In the next section, capacity design considerations specific to coupled walls are discussed, along with the existing capacity design approaches to be studied. Following this, the numerical modelling and NTHA of the case study structure is examined. The NTHA results are then compared to the capacity design predictions and the performance of each method evaluated. Finally, conclusions are drawn and recommendations made for future research.

---

[1] PhD Candidate, ROSE Programme, UME Graduate School, IUSS Pavia, Italy, matthew.fox@umeschool.it
[2] Assistant Professor, University of Pavia, Italy, timothy.sullivan@unipv.it
[3] Assistant Professor, École Polytechnique Fédérale de Lausanne, Switzerland, katrin.beyer@epfl.ch

CASE STUDY BUILDING

The case study building to be examined in this work is shown in Fig.1. It is 10 storeys high and each storey has a height of 3.4m. The plan dimensions of each level are 30m by 30m and the seismic mass of each level is calculated to be 460t. In the direction being considered, coupled walls on opposite sides of the building are used to resist lateral loads. Each set of coupled walls is symmetric, with the walls being 4m long and 0.25m thick. The coupling beams are 0.2m thick, 0.8m deep and have a span of 2m. Characteristic strength values of 30MPa for concrete and 400MPa for reinforcing are used.
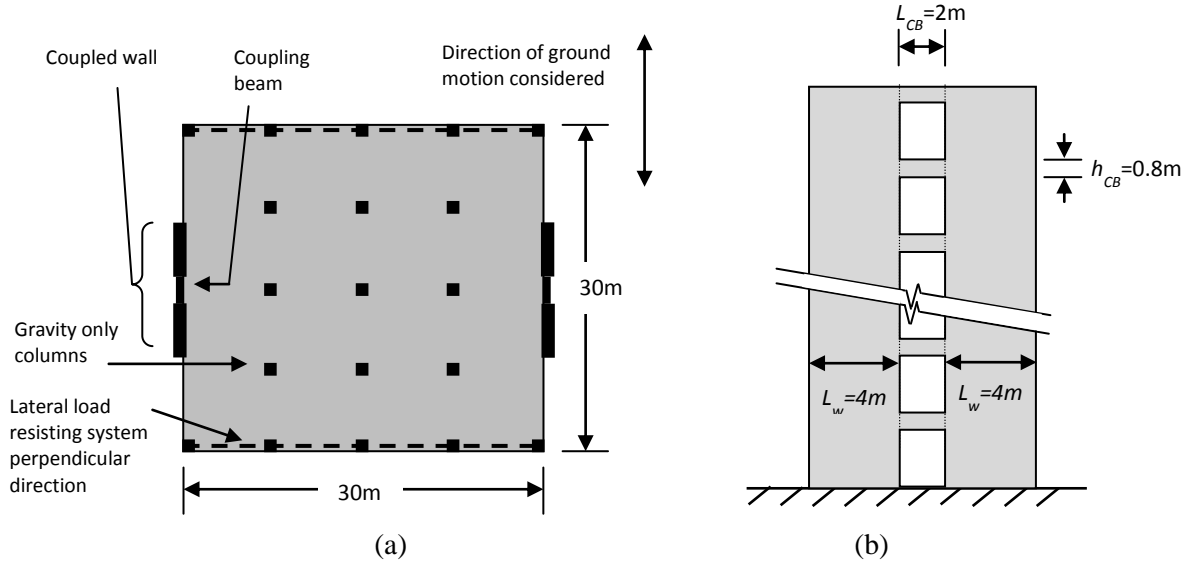

Figure 1. (a) Plan view of case study building. (b) Elevation of a coupled wall.

The seismic design of the building was carried out using Direct Displacement-Based Design (DDBD) (Priestley *et al.*, 2007); however, specific aspects of the procedure relating to coupled walls were updated to match the model code DBD12 (Sullivan *et al.*, 2012) and the work of Fox *et al.* (2014a). An up to date step-by-step guide is provided in Fox *et al.* (2014a). The coupling beams are designed using diagonal reinforcing due to the superior deformation capacity of this arrangement (Paulay and Binney, 1974; Paulay and Santhakumar, 1976); however, this work is equally applicable to coupled walls using conventional coupling beam reinforcing, provided that they exhibit sound behaviour under reversed cyclic loading.

DDBD allows the designer to choose, within limits, how strength is distributed to the different plastic regions within the structure. For coupled walls this requires the designer to make two choices. The first is the selection of an appropriate coupling ratio, β, which defines what portion of the overturning moment is resisted by the axial force couple generated in the walls. This is defined in Eq.(1).

$$\beta = \left(\sum_{i=1}^{n} V_{CBi}\right)(L_{CB} + L_{W})/M_{OTM} \qquad (1)$$

where V_{Cbi} is the shear strength of coupling beam i and M_{OTM} is the total overturning moment. For the design of the case study structure a coupling ratio of 0.3 was chosen, this is considered to be a moderate level of coupling. Caution should be taken as too higher coupling ratio may cause excessive axial forces in the walls, on the other hand selecting a very low coupling ratio provides little benefit in terms of resisting seismic loads.

The design was carried out for the type 1 spectrum in Eurocode 8 (EC8) (CEN, 2004) for ground type C and a reference ground acceleration of a_g=0.3g, but with the displacement spectrum corner period, T_D, extended out to 8s. The longer corner period is used as the current EC8 value of

T_D=2s is unconservative for large magnitude events. For this reason, in the absence of a better estimate of the corner period, the rather long period of 8s was chosen. The acceleration and displacement spectra are shown in Figs.2(a) & (b) respectively. Overlaid are the response spectra for the set of 10 accelerograms (see Appendix for details) used in the NTHA, which are discussed further in the corresponding section. All design and response spectra are computed for 5% damping.
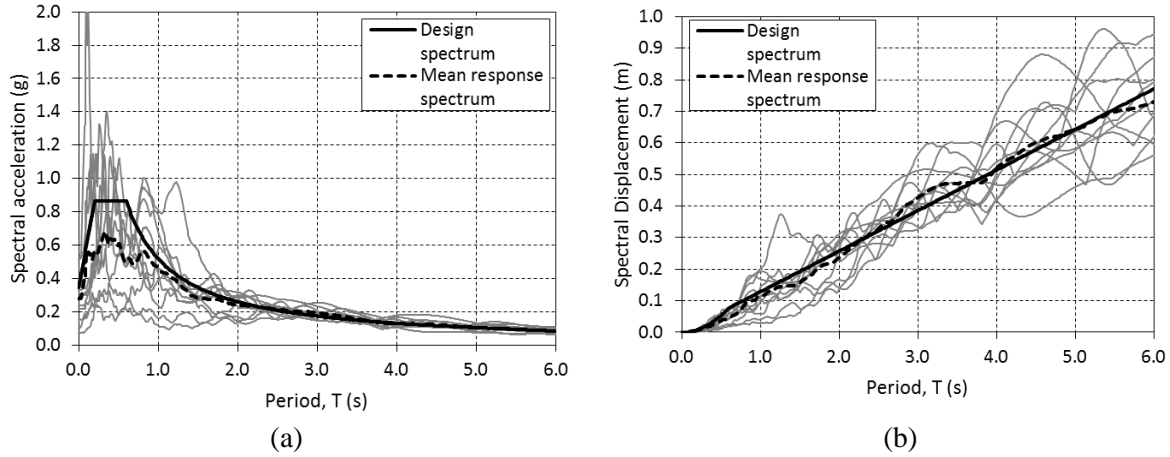

Figure 2. Design and response spectra for (a) acceleration and (b) displacement.

Key outputs from the DDBD procedure are provided in Table.1, where Δ_d is the displacment of the equivalent single-degree-of-system, V_B is the design base shear, μ_{sys} is the system displacement ductility and T_1 and T_e are the initial period of effective period of the structure respectively. It should be noted that the initial period is calculated with *EI* determined from the section secant stiffness to yield.

Table 1. Design output from DDBD

Δ_d (m)	0.468
V_B (kN)	2230
M_{OTM} (MNm)	54.9
μ_{sys}	4.92
T_1 (s)	2.2
T_e (s)	5.68

EXISTING CAPACITY DESIGN APPROACHES

A key aspect of capacity design is predicting the maximum actions that can be developed in regions of the structure where non-ductile failure can occur. For coupled walls, plastic hinges form at the base of the walls and in the coupling beams (although not strictly a hinge as yielding occurs along the full length of the diagonal reinforcing). Therefore, capacity design must be used to design against shear failure up the full height of the walls and against flexural failure above the plastic hinge region. To determine the maximum forces that can develop in these regions, the designer must account for material overstrength, higher mode effects, compatibility forces and 3D-effects. The first of these is rather straight forward and accounted for through an overstrength factor, ϕ^o, to increase the design actions. Higher mode effects are accounted for in various different ways and will be discussed in detail in reference to each different capacity design approach. Compatibility forces are not discussed in detail in this paper; however, the interested reader is referred to Beyer *et al.* (2014), which provides an example for the case of walls with different lengths, connected by rigid diaphragms. Likewise, 3D-effects such as slab coupling and the influence of transverse beams are not covered, but the reader is referred to Sullivan (2010).

EC8 Approach

The first of the capacity design approaches to be considered is that of EC8 (CEN, 2004). To ensure that flexural yielding does not occur above the plastic hinge region it is necessary to follow the requirements of clause *5.4.2.4(5)*, which requires the designer to amplify the bending moments found from elastic analysis. For coupled walls, the bending moment diagram (in first mode response) changes sign up the height of the walls, with the contraflexure height being a function of the coupling ratio. Therefore, for coupled walls it seems appropriate that the provisions for dual systems (*i.e.* frame-wall systems) be applied, rather than the provisions for cantilever walls. As is shown in Fig.3, the design bending moment diagram is constructed from a straight line that encloses the bending moment diagrams from analysis in each direction. An allowance for tension shift should then be made; however, in this work the effects of tension shift are neglected due to the difficulties associated with capturing this behaviour in a numerical model. It is important to note that this approach is independent of earthquake intensity.
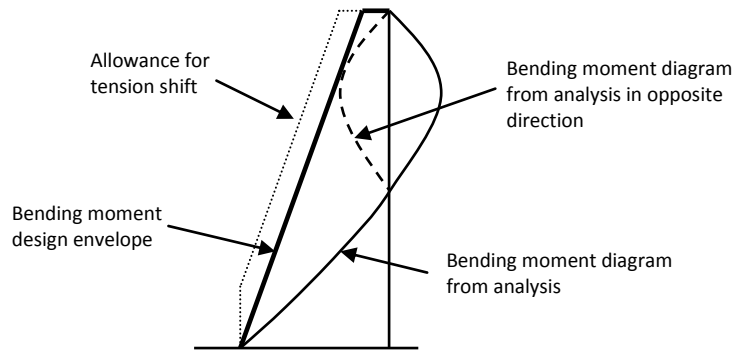

Figure 3. Bending moment design envelope for dual systems in accordance with EC8 (figure adapted from EC8 (CEN, 2004))

Capacity design for shear forces in accordance with EC8 differs for Ductility Class Medium (DCM) and Ductility Class High (DCH) structures. For DCM structures the design shear forces are obtained by increasing the shear forces from analysis by 50%. For DCH structures the shear forces from analysis should be multiplied by the factor ε, given by Eqn.(2).

$$\varepsilon = q\sqrt{\left(\frac{\gamma_{Rd}}{q}\cdot\frac{M_{Rd}}{M_{Ed}}\right)^2 + 0.1\left(\frac{S_e(T_C)}{S_e(T_1)}\right)^2} \leq q \qquad (2)$$

where γ_{Rd} is the overstrength factor to account for strain-hardening, M_{Rd} is the design moment resistance, q is the reduction factor, which is taken as the system ductility, μ_{sys}, and $S_e(T_C)$ and $S_e(T_1)$ are the ordinates of the elastic design acceleration spectrum at the corner period (of the acceleration spectrum), T_C, and the fundamental period of the structure respectively.

Priestley et al. (2007) approach

Priestley *et al.* (2007) provide a set of equations for the capacity design of cantilever walls, which they state can be conservatively extended to the capacity design of coupled walls. In the capacity design for flexure, the design bending moment envelope is constructed as a bilinear curve between the overstrength moment demand at the base of the wall, $\phi^o M_B$, the mid-height moment, $M^o_{0.5Hn}$, and zero at roof level. The mid-height moment demand is calculated from Eqn.(3).

$$M^o_{0.5Hn} = C_{1,T}\phi^o M_B, \quad \text{where} \quad C_{1,T} = 0.4 + 0.075T_i\left(\frac{\mu}{\phi^o}-1\right) \geq 0.4 \qquad (3)$$

4

ϕ^o is the overstrength factor and T_i is the initial period of the structure. Again tension shift should be accounted for, but in this work is ignored for reasons mentioned previously.

The shear force capacity design envelope is constructed as a linear envelope between the capacity design shear force calculated at the base of the wall, V^o_{Base}, and at roof level, V^o_n, which are calculated from Eqns.(4)-(6).

$$V^o_{Base} = \phi^o \omega_V V_{Base} \text{ , where} \qquad (4)$$

$$\omega_V = 1 + \frac{\mu}{\phi^o} C_{2,T} \quad \text{and} \quad C_{2,T} = 0.067 + 0.4(T_i - 0.5) \leq 1.15 \qquad (5)$$

$$V^o_n = C_3 V^o_{Base} \quad \text{where} \quad C_3 = 0.9 - 0.3 T_i \geq 0.3 \qquad (6)$$

It should be noted that the equations for both bending moments and shear forces account for earthquake intensity through the incorporation of the ductility factor, μ. It has however been argued by Sullivan (2010) that ductility demand might not be the best parameter to measure intensity since it does not account for spectral shape and therefore may not adequately capture the relative intensity of higher modes. Priestley *et al.* (2007) make no specific recommendation on which ductility value should be used in Eqns.(3) & (5), with the different possibilities being the wall ductility demand, μ_{wall}, the average coupling beam ductility demand, μ_{CB}, or the overall system ductility demand, μ_{sys}. For dual wall frame structures the use of μ_{sys} has been recommended, but in this research it was found that for coupled walls the use of the system ductility led to very poor results. Therefore, it is recommended that the wall ductility demand be used instead.

Fox et al. (2014b) approach

Fox *et al.* (2014b) provide capacity design recommendations specifically for coupled walls. For flexure a rather alternative approach is taken. It was recognised that exceeding the moment capacity in the upper regions of a wall (where ductile detailing is not provided) is unlikely to lead to catastrophic failure and therefore some low-level yielding should be permissible. An upper limit for curvature ductility is tentatively set at $\mu_\phi=3$, which corresponds to the curvature ductility at which the concrete contribution to shear resistance in the modified UCSD model (Kowalsky and Priestley, 2000) begins to reduce. It was found that by using constant longitudinal reinforcing up the full height of the wall the maximum curvature ductility could be kept below $\mu_\phi=3$. Curtailment of flexural reinforcing is then permitted in the top 30% of the wall, but ensuring that the moment capacity at roof level is greater than the value given by Eqn.(7) in which *n* is the number of stories.

$$M_{roof} = \phi^o \frac{\beta.M_{OTM}}{2n} \qquad (7)$$

The Fox *et al.* (2014b) approach to capacity design shear forces is based on the work of Pennucci *et al.* (2011) and provides a simplified set of equations that could be easily incorporated into a design code. The Pennucci *et al.* (2011) approach considers the evolution of ductility throughout the coupled wall system as earthquake intensity increases, as shown in Fig.4. At low intensities the structure remains elastic (Fig.4(a)), then as intensity increases, the coupling beams yield. Because ductility demand on the coupling beams is typically very high, they can be assumed to act as pinned at each end (Fig.4(b)). Further increases in intensity lead to yielding at the base of the walls and eventually (for what regards higher mode effects) the structure can be assumed to behave like two pinned base cantilevers. The shear forces due to each mode are calculated separately and then combined using SRSS. For higher modes, the shear forces are obtained from the equations for cantilevers of constant stiffness with constant distributed mass and it is assumed the fixity at their base is somewhere between fixed and pinned (dependent on ductility demand).
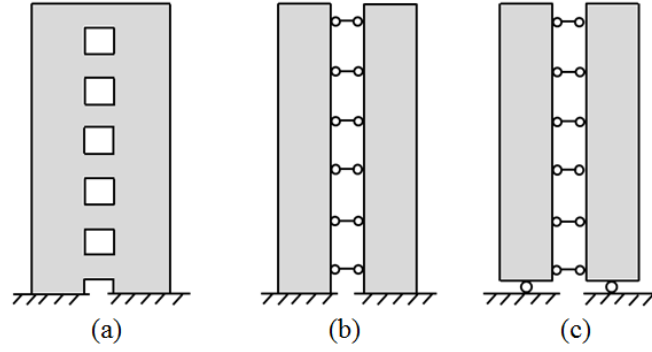
Figure 4. Evolution of ductility in a coupled wall system (a) low, (b) medium and (c) high intensities, adapted from Pennucci *et al.* (2011).

Only the shear forces at the base of the wall and mid-height are needed to construct the shear force envelope, which varies linearly from the base of the walls to mid-height and then remains constant up to roof level. The application of this method was shown by Pennucci *et al.* (2011) to give very accurate results.

Fox *et al.* (2014b) identified that the Pennucci *et al.* (2011) approach could be simplified significantly and put into a convenient set of equations with minimal reduction in accuracy. The base shear and mid-height shear are calculated from Eqns.(8)-(12) and the shear force envelope is constructed in the manner described previously for the Pennucci *et al.* (2011) approach.

$$V_{Base}^o = \sqrt{\left(\phi^o V_{Base}\right)^2 + C_2 \left(m.Sa_{PL}\right)^2} \tag{8}$$

$$V_{m-h}^o = \sqrt{\left(0.85\phi^o V_{Base}\right)^2 + C_3 \left(m.Sa_{PL}\right)^2} \tag{9}$$

$$C_1 = \frac{2T_C^2 EI}{mH_n^3} \tag{10}$$

$$C_2 = \min \begin{cases} 0.048 - 0.008\mu \\ \\ \left(0.56 - 0.125\mu\right)\left(C_1 + 0.01\right) \end{cases} \tag{11}$$

$$C_3 = \min \begin{cases} 0.022 + 2\times10^{-4}\mu \\ \\ \left(0.0019\mu - 2.8\times10^{-4}\right)C_1 + 0.0026 \end{cases} \tag{12}$$

where V_{m-h}^o is the capacity design shear at mid-height, Sa_{PL} is the spectral acceleration on the spectrum plateau, m is the total tributary mass of the coupled wall system and μ is the wall ductility demand.

The Fox *et al.* (2014b) approach, along with that of Pennucci *et al.* (2011), accounts for the following important phenomena:

- Relationship between higher mode effects and earthquake intensity through the use of the Sa_{PL} term.
- Influence of spectral shape on higher mode effects through the C_1-C_3 coefficients.
- Influence of ductility on higher mode response through the incorporation of μ.

NUMERICAL MODELLING

A numerical model of the case study structure was constructed using the program SeismoStruct v6.5 (Seismosoft, 2013) and a number of nonlinear time-history analyses conducted at varying intensity levels. A screen shot of the numerical model is given in Fig.5. To model the walls, distributed plasticity fibre-section elements were chosen. As the nonlinear material stress-strain relationships are included on a sectional level, the elements can implicitly account for axial force-moment interaction. Moreover, the member elongation that occurs in an RC member subject to flexure is captured. This is important in the analysis of coupled walls as differential wall elongation affects the rotation demands on the coupling beams. A displacement-based element formulation was used, with the base element being equal to the plastic hinge length (see Yazgan and Dazio, 2010) and it should be noted that force-based elements were not employed as they tend to significantly over-estimate curvature demands at the base of walls.
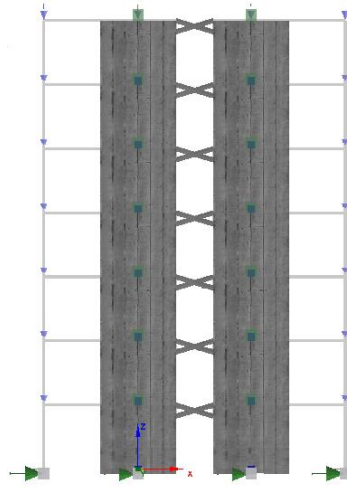

Figure 5. SeismoStruct (Seismosoft, 2013) screenshot of numerical model.

The diagonally reinforced coupling beams were modelled using a set of fibre-section truss elements arranged in a diagonal configuration. This modelling strategy was shown in Fox *et al.* (2014a) to accurately capture the behaviour a diagonally reinforced coupling beam subjected to reverse cyclic loading. It should be noted that interaction between the coupling beam and the floor slab has been neglected in this work due to uncertainty associated with modelling this effect. As the floor slab is neglected in both design and analysis it is not expected to affect the outcomes of this research; however, this is certainly something that cannot be neglected in the design and analysis of real buildings.

The distributed plasticity beam elements in SeismoStruct are rigid in shear and it was therefore necessary to implement additional transverse springs between the wall elements at each floor level. Although the shear stiffness of ductile walls is nonlinear, previous studies on cantilever walls showed that linear springs yield reasonable estimates of the system's base shear (Beyer *et al.*, 2014). The stiffness of the springs was determined using Eqn.(13) from Beyer *et al.* (2011). The equation is semi-empirical and accounts for experimental evidence showing that the ratio of shear to flexural deformations in capacity designed walls remains relatively constant (Dazio *et al.*, 2009).

$$\frac{\Delta_s}{\Delta_f} = 1.5 \frac{\varepsilon_m}{\phi \tan \beta_{cr}} \frac{1}{H_n} \tag{13}$$

where Δ_s and Δ_f are the shear and flexural deformations respectively, ϕ is the curvature, ε_m is the mean axial strain, β_{cr} is the maximum crack inclination (assumed to be 45°) and H_n is the shear span.

Tangent stiffness proportional damping was employed with 2% of critical damping specified at the period corresponding to the first elastic mode of vibration. This decision was based on

recommendations in literature (Priestley and Grant, 2005). The choice of 2% of critical damping was considered to be a compromise between the 5% typically assumed for reinforced concrete buildings and 0% as recommended by Petrini *et al.* (2008) for use with fibre-section models (although note that the recommendations made by Petrini *et al.* (2008) related to experimental testing of a bridge pier on a shake table and therefore excluded some sources of damping).

For the NTHA the numerical model was subjected to a set of 10 ground motions from Maley *et al.* (2013). The response spectra for each ground motion are shown in Fig.2. It will be noted that the mean response spectrum is significantly lower than the design spectrum in the period range from 0.2 to 0.8s. This was the result of selecting records specifically for DDBD with a focus on the longer period range. To account for this in the Fox *et al.* (2014b) approach the maximum spectral acceleration was taken as 0.6g.

COMPARISON OF NTHA RESULTS AND CAPACITY DESIGN PREDICTIONS

Fig.6 shows the mean maximum shear forces obtained from NTHA and the shear forces predicted using the different capacity design approaches. Two different intensity levels were considered; 100% of the design intensity (Fig.6(a)) and 150% of the design intensity (Fig.6(b)), the latter could be considered to roughly correspond to the maximum credible event at the site. Note that it is the total shear force in the coupled wall system that is shown, rather than the shear force in an individual wall.
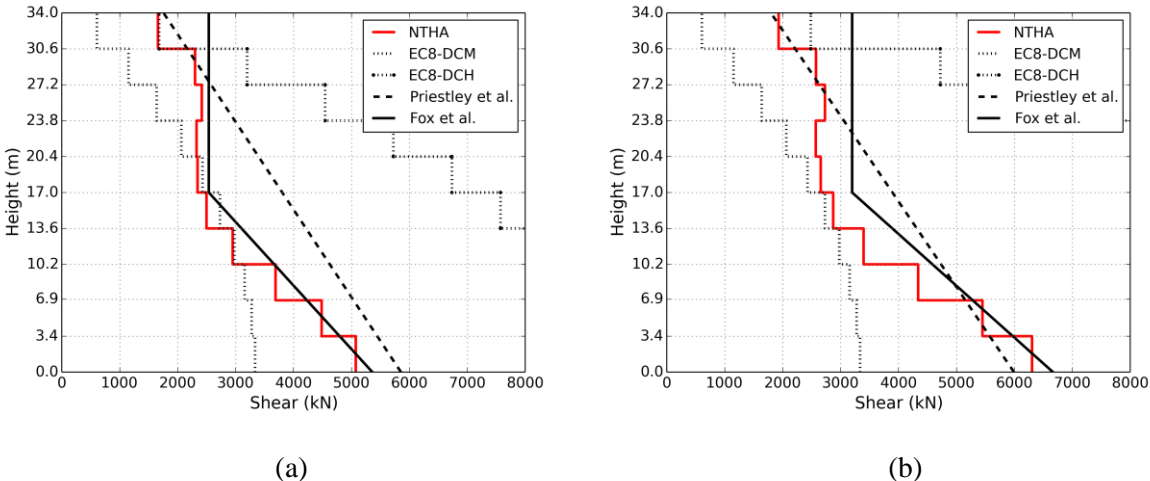

Figure 6. Comparison of mean maximum shear forces from NTHA and capacity design predictions at (a) 100% and (b) 150% of the design intensity.

Similar trends can be observed at both intensity levels. The EC8 approach generally provides a poor fit to the NTHA results. For DCM the capacity design shear forces are significantly unconservative, while for DCH the shear forces are far too conservative. As the EC8 approach (for DCM and DCH) linearly scales the fundamental mode shear forces it is clear that it will never predict the shear profile up the height of structure to a high degree of accuracy. The Priestley *et al.* (2007) approach gives accurate predictions of the shear forces at the base of the walls and at roof level; however, the linear envelope between these two points does not fit particularly well and is rather conservative around mid-height. The Fox *et al.* (2014b) approach gives an excellent fit at the design intensity, but at 150% of the design intensity tends to give rather conservative results, particularly in the upper half of the building. Of all the shear force profiles up the height of the structure it is clear that the Fox *et al.* (2014b) approach best matches the NTHA results.

To assess the performance of the EC8 and Priestley *et al.* (2007) approaches for flexural capacity it was necessary to restrict yielding of the walls in the numerical model to only the plastic hinge regions. To achieve this (at least in an approximate sense) the wall reinforcing above the plastic hinge region was set to be linear elastic. The resulting bending moment profiles along with the capacity design predictions are shown in Fig.7 for the design intensity (Fig.7(a)) and 150% of the

design intensity (Fig.7(b)). Note that it is the sum of the bending moments carried by both walls that is shown, rather than the maximum bending moment in a single wall.

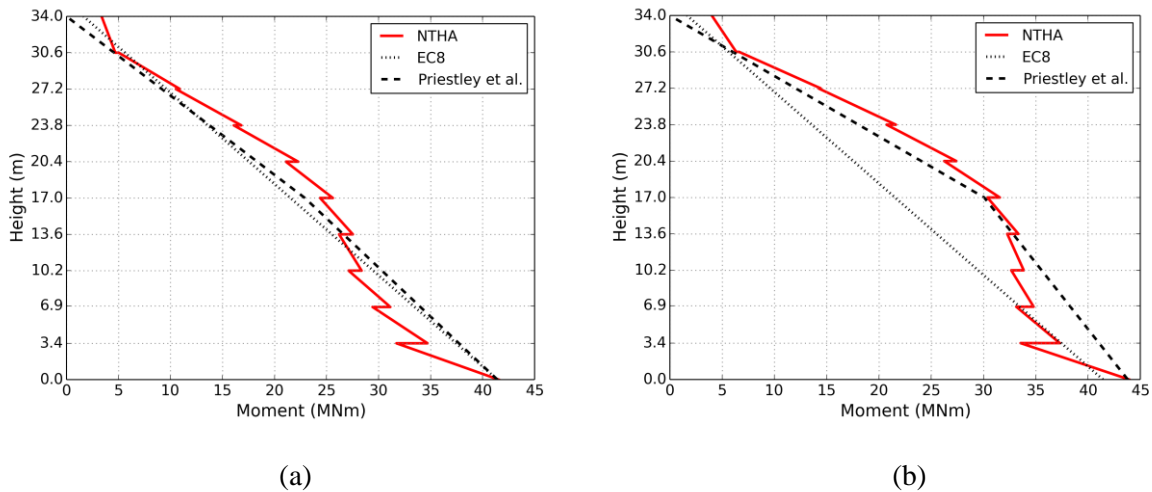(a)   (b)

Figure 7. Comparison of mean maximum bending moments from NTHA and capacity design predictions at (a) 100% and (b) 150% of the design intensity.

It can be observed that the EC8 capacity design bending moment profile gives a reasonable prediction of the NTHA bending moments at the design intensity. However, as the intensity increases, there is a significant increase in the NTHA bending moments around mid-height of the building. As the EC8 approach is independent of intensity, it is unable to capture this increase and is significantly unconservative. The Priestley *et al.* (2011) approach is able to give a reasonably good estimate of the bending moments at both intensity levels, although in each case is slightly on the unconservative side. A problem now arises when computing the reinforcing to be provided to each wall individually. As the axial loads in each individual wall vary (due to the coupling effect) it is not clear which point on the moment-axial force interaction curve will be critical. A safe option would be to provide reinforcing to resist the maximum bending moment while assuming the minimum axial compression force is acting; however, this may be excessively conservative. This dilemma promotes that alternative approach of Fox *et al.* (2014b) to be discussed next.

Fig.8 shows the maximum wall curvatures up the height of the building. In this case the numerical model used in the NTHA was set with the true reinforcing properties up the height and was thus free to yield at any location.

(a)   (b)
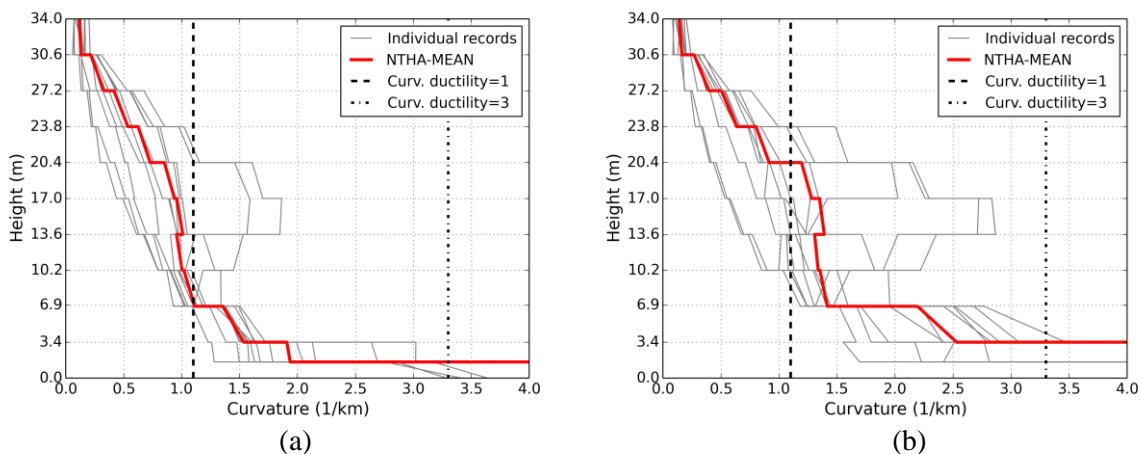
Figure 8. Comparison of curvature profiles from NTHA and capacity design predictions at (a) 100% and (b) 150% of the design intensity.

From Fig.8 it can be observed that at the design intensity the walls (on average) do not yield above the plastic hinge region. However, at 150% of the design intensity low-level yielding occurs over a number of levels above the plastic hinge region. Therefore, it can be concluded that for this case study structure, to achieve the conventional capacity design objective of preventing yielding outside of

the plastic hinge region, it would be necessary to provide more reinforcing in the upper regions of the wall than at the base. Although this is a sound engineering option it could seem unconventional to practicing design engineers. Therefore, by simply keeping the reinforcing constant up the full height of the wall, as per Fox et al. (2014b), some low-level yielding may occur, but is unlikely to significantly impact on the performance of the structure.

SHEAR FORCES IN INDIVIDUAL WALLS

In the previous section, shear forces were investigated in terms of the total shear force in the coupled wall system. However, for a designer to calculate the required quantity of shear reinforcing it is necessary to know the capacity design shear force acting on an individual wall. The common approach, as for example in EC8, is to redistributed the shear forces in proportion to moment redistribution at the base of the walls. However, it was found by Fox et al. (2014b) that this was unnecessarily conservative and is demonstrated in Fig.9. The line labelled 'NTHA- individual wall' is the maximum shear force taken directly from an individual wall during the NTHA, the line labelled 'NTHA –proportioned total' is the total shear force in the coupled wall system (found from NTHA) multiplied by the ratio of the maximum base moment in an individual wall to the maximum sum of the moments in both walls.
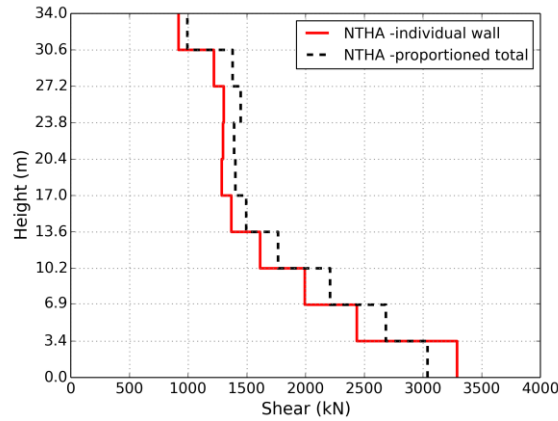

Figure 8. Maximum shear forces in individual walls found directly from NTHA and from the proportioned total shear.

It should be noted that in this case the difference is not particularly significant due to the low coupling ratio, but as the coupling ratio increases this effect can become more severe. Fox et al. (2014b) reasoned that the shear force due to the fundamental mode could be distributed in proportion to the bending moment at the base of the walls, but the shears due to higher modes should be split more evenly. They proposed the following equations (replacing Eqns.(8) and (9)) to find the shear forces in individual walls:

$$V_{base} = \sqrt{\left(\frac{M_C}{M_C + M_T}\phi^o V_d\right)^2 + C_2\left(0.55 m.Sa_{PL}\right)^2} \tag{14}$$

$$V_{m-h} = \sqrt{\left(\frac{0.85 M_C}{M_C + M_T}\phi^o V_d\right)^2 + C_3\left(0.5 m.Sa_{PL}\right)^2} \tag{15}$$

where M_C and M_T are the wall moments under maximum axial compression and tension forces respectively.

Fig.8 also exhibits the effects of the compatibility forces. There is a significant jump in the shear force in the bottom level of the building, which is due to the elongation of the coupling beam at level 1. As the coupling beam elongates its lengthening is resisted by the walls being pushed apart. An increase in shear force in the compression wall is therefore observed, accompanied by a decrease in shear force in the tension wall. Quantifying the effects of the compatibility forces should be studied in future research.

CONCLUSIONS

This research has investigated the performance of three different approaches for the capacity design of RC coupled walls; those of EC8 (CEN, 2004), Priestley *et al.* (2007) and Fox *et al.* (2014b). To assess the performance of each approach the capacity design predictions were assessed against the results of nonlinear time-history analyses conducted using a distributed plasticity fibre-section element model. The approaches of Priestley *et al.* (2007) and Fox *et al.* (2014b) were shown to accurately predict the shear forces in the coupled wall system, while the EC8 approach was unconservative for DCM and too conservative for DCH.

The Priestley *et al.* (2007) approach was shown to give a reasonable prediction of capacity design bending moments in the upper regions of the wall. The EC8 approach gave a good prediction at the design intensity, but as the approach is intensity independent it was insufficient at 150% of the design intensity. It was reasoned that a more practical approach to flexural capacity design could be to control curvatures rather than moments. The recommendation of Fox *et al.* (2014b) to use constant reinforcing up the height of the wall was found to keep curvature ductlities below a low limit.

It was also shown how the maximum shear forces in the individual wall can be related to the maximum shear forces in the coupled wall system and that distributing shear forces in proportion to moment resistances at the base of the walls (accounting for the varying axial loads) is conservative.

For future research the three following areas are seen as the most important; (i) accounting for coupling beam-floor slab interaction, (ii) determining appropriate curvature limits for the upper regions of a wall where ductile detailing is not provided, and (iii) quantifying the effects of compatibility forces associated with coupling beam elongation.

ACKNOWLEDGMENTS

REFERENCES

Beyer K, Dazio A and Priestley MJN (2011) "Shear deformations of slender reinforced concrete walls under seismic loading," *ACI Structural Journal*, 108(2):167-177.

Beyer K, Simonini S, Constantin R and Rutenburg A (2014) "Seismic shear distribution among interconnected cantilever walls of different lengths," *Earthquake Engineering and Structural Dynamics*, published online DOI 10.1002/eqe.2403.

Comité Européen de Normalisation (2004) Eurocode 8, Design of Structures for Earthquake Resistance – Part 1: General Rules, Seismic Actions and Rules for Buildings, EN 1998-1, CEN, Brussels, Belgium.

Dazio A, Beyer K, Bachmann H (2009) "Quasi-static cyclic tests and plastic hinge analysis of RC walls," *Engineering Structures*, 31(7):1556-1571.

Fox MJ, Sullivan TJ and Beyer K (2014a) "Comparison of force-based and displacement-based design approaches for RC coupled walls in New Zealand," *Bulletin of the New Zealand Society for Earthquake Engineering*, submitted.

Fox MJ, Sullivan TJ and Beyer K (2014b) "Capacity design of coupled RC walls," *Journal of Earthquake Engineering*, 18(5): 735-758.

Kowalsky MJ and Priestley MJN (2000) "An improved analytical model for shear strength of circular RC columns in seismic regions," *ACI Journal*, 97(3):388-396.

Maley TJ, Sullivan TJ, Lago A, Roldán R and Calvi GM (2013) <u>Characterising the Seismic Behaviour of Steel MRF Structures</u>, EUCENTRE Research Report 2013/2, IUSS Press, Pavia, Italy.

Park R and Paulay T (1975) <u>Reinforced Concrete Structures</u>, Wiley, New York, United States of America.

Paulay T and Binney JR (1974) "Diagonally reinforced coupling beams of shear walls," *Publication SP-42*, American Concrete Institute, 579-598.

Paulay T and Priestley MJN (1992) <u>Seismic Design of Reinforced Concrete and Masonry</u>, Wiley, New York, United States of America.

Paulay T and Santhakumar R (1976) "Ductile behaviour of coupled shear walls," *Journal of the Structural Division, Proceedings of the American Society of Civil Engineers*, 102(ST1):1006-1014.

Pennucci D, Sullivan TJ and Calvi GM (2011) <u>Performance-Based Seismic Design of Tall RC Wall Buildings</u>, Rose Research Report 2011/02, IUSS Press, Pavia, Italy.

Petrini L, Maggi C, Priestley MJN, Calvi GM (2008) "Experimental verification of viscous damping modeling for inelastic time history analyzes [sic]," *Journal of Earthquake Engineering*, 12(SP1):125-145.

Priestley MJN, Calvi GM and Kowalsky MJ (2007) <u>Displacement-Based Seismic Design of Structures</u>, IUSS Press, Pavia, Italy.

Priestley MJN and Grant DN (2005) "Viscous damping in seismic design and analysis," *Journal of Earthquake Engineering*, 9(SP2):229-255.

Seismosoft (2013) "SeismoStruct – A computer program for static and dynamic nonlinear analysis of framed structures," Available from URL: www.seismosoft.com.

Sullivan TJ (2010) "Capacity design considerations for RC frame-wall structures," *Earthquakes and Structures*, 1(4):1-20.

Sullivan TJ, Priestley MJN and Calvi GM (Editors) (2012) <u>A Model Code for the Displacement-Based Seismic Design of Structures DBD12</u>, IUSS Press, Pavia, Italy.

Yazgan U and Dazio A (2010) "Critical aspects of finite element modeling of RC structures for seismic performance assessment," *Proceedings of the 9th U.S. National and 10th Canadian Conference on Earthquake Engineering*, Paper No. 404, Toronto, Canada.

Appendix

The following accelerograms were used in the nonlinear time-history analyses.

Earthquake Name	Station Name	M_W	r (km)	Scale Factor	V_{S30} (s)	Duration (s)
Chi-Chi	CHY082	7.6	36	1.6	194	90
Kocaeli	KOERI Botas	7.5	127	5.9	275	102
Landers	CDMG 14368 Downey	7.3	157	3.0	272	70
Hector	Mecca-CVWD Yard	7.1	92	2.2	345	60
St Elias	USGS 2728 Yakutat	7.5	80	1.2	275	83.2
Loma Prieta	USGS 1028 Hollister City Hall	6.9	28	1.4	199	39.1
Northridge-01	Neenach-Sacatara Ck	6.7	52	4.3	309	48
Superstition Hills-02	Westmorland Fire Sta	6.5	13	1.7	194	40
Imperial Valley-06	El Centro Array #1	6.5	22	3.8	237	39.3
Chi-Chi-03	TCU061	6.2	40	4.2	273	107